Organic & Biomolecular Chemistry

www.rsc.org/obc

Volume 10 | Number 6 | 14 February 2012 | Pages 1125–1312

ISSN 1477-0520

RSC Publishing

PAPER

Zeng *et al*.

Synthesis, structural investigation and computational modelling of water-binding aquafoldamers

1477-0520(2012)10:6;1-H

Organic & Biomolecular Chemistry

Dynamic Article Links

Cite this: *Org. Biomol. Chem.*, 2012, **10**, 1172

www.rsc.org/obc

PAPER

Synthesis, structural investigation and computational modelling of water-binding aquafoldamers†

Huaiqing Zhao,[a] Wei Qiang Ong,[a] Xiao Fang,[a] Feng Zhou,[b] Meng Ni Hii,[a] Sam Fong Yau Li,[a] Haibin Su[b] and Huaqiang Zeng*[a]

Received 21st September 2011, Accepted 31st October 2011
DOI: 10.1039/c1ob06609a

Detailed studies on water-binding aquafoldamers are presented that illustrate the potential use of the elongated larger aquafoldamers for recognizing larger water clusters of diverse topologies. A novel self-trapping dimerization mode involving two tetramer molecules is proposed, which is consistent with the obtained varying experimental evidences.

Introduction

Aquaporins are a group of specialized transmembrane proteins that form a hydrophobic pore system across the cell membrane.[1] Four of these proteins, in the tetrameric form, form a water channel across the lipid bilayer allowing for the transportation of water molecules, in a 1D chain-like arrangement, across the membrane.[2] The possible use of water-transporting aquaporins for wastewater reclamation and re-use as well as seawater desalination is being investigated industrially by a company called Aquaporin. However, significant challenges associated with manipulating channel proteins in terms of complexity, stability, availability and activity reconstitution still exist. An alternative strategy is to design small molecule-based synthetic water channels that can mimic aquaporins to a certain degree of related functionality for various applications including water purification. Toward this goal, we have been interested in designing water-binding aquafoldamers as illustrated by oligoamides **1–5**[3] with an ultimate aim to realize synthetic water channels for rapid, efficient transportation of water molecules while excluding all the other molecular species.

There have been a few different approaches to mimic the aquaporin water channel, namely using supramolecular[4] and metal–organic framework approaches.[5] These water hosts have usually relied on conformationally more flexible organic or organometallic molecules with respect to foldamers whose well defined backbones are primarily stabilized by non-covalent forces such as π–π stacking interactions, solvophobic forces and H-bonds. Interestingly, despite their great diversities,[6] only a few foldamer molecules of similar type have been reported by Lehn and Huc.[7] Some of these bio-inspired water hosts had also been shown to be able to host a 1D helical chain of water molecules in their framework, reminiscent of aquaporins. Here we describe our approach using pyridine-based aquafoldamers **1–5** that fold into a crescent structure to enclose a defined water-binding cavity by intramolecular H-bonding networks.[9,10] The elongated aquafoldamers with sufficiently long enough backbones may function as synthetic water-transporting channels. In this article, detailed characterization of water-binding aquafoldamers composed of up to five repeating units were carried out using X-ray crystallography, variable-temperature ^{1}H NMR experiments, 2D NOESY studies and *ab initio* molecular modelling.

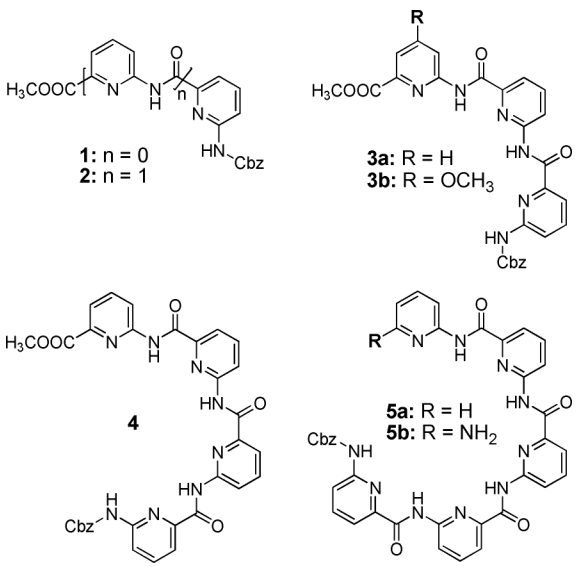

Results and discussion

Synthesis of aquafoldamers 1–5

We recently reported our studies on the pyridine-based foldamers **2–4** and **5a**,[3] demonstrating that with an increasing addition

[a]*Department of Chemistry, National University of Singapore, 3 Science Drive 3, Singapore. E-mail: chmzh@nus.edu.sg; Fax: (+) 65-6779-1691; Tel: (+) 65-6516-2683*

[b]*Division of Materials Science, 50 Nanyang Avenue, Nanyang Technological University, Singapore, 639798*

† Electronic supplementary information (ESI) available. CCDC reference number 834710. For ESI and crystallographic data in CIF or other electronic format see DOI: 10.1039/c1ob06609a

of the pyridine-based building blocks, the elongated backbone becomes increasingly curved in one direction as a result of the stabilizing forces from the progressively lengthened intramolecular H-bonding network.[10] This new class of aromatic foldamers closely mimics the helicity requirement by π-helices where about 4.3 units are required for each helical turn. This value also closely resembles the tetrameric arrangement of the aquaporin required to furnish a water channel in the membrane. All the aquafoldamers described in Scheme 2 were synthesized from commercially available pyridine-2,6-dicarboxylic acid (**1a**) and diethyl oxalate (**1f**) after up to 12 steps with an overall yield of about 1% for pentamers **5a** and **5b**.

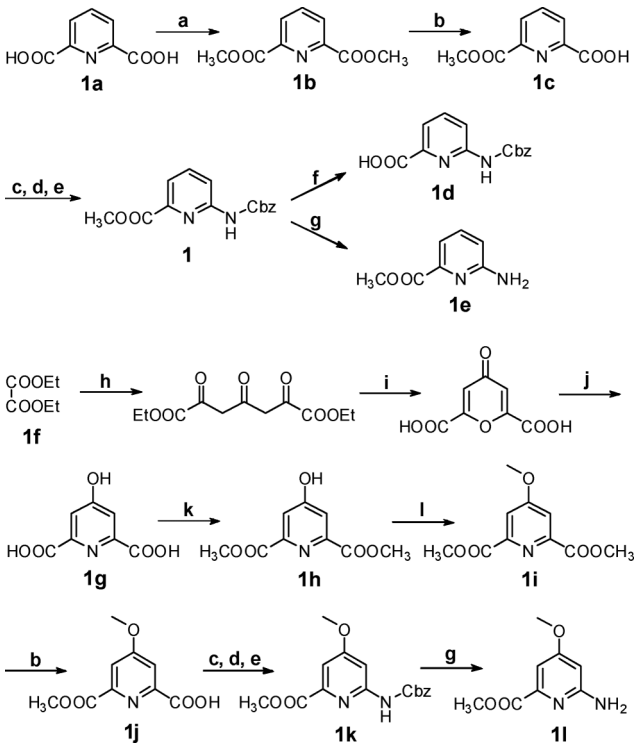

Scheme 1 Synthesis of monomeric building blocks. *Reagents and conditions*: (a) conc. H_2SO_4, MeOH, reflux; (b) KOH, MeOH; (c) 4-methylmorpholine, ethyl chloroformate, THF–DMF, −10 to 0 °C; (d) aq. NaN_3; (e) BnOH, toluene, reflux; (f) NaOH, dioxane; (g) Pd/C, H_2, THF; (h) sodium ethoxide, then acetone; (i) conc. HCl; (j) 10% aq. NH_3; (k) $SOCl_2$, MeOH; (l) K_2CO_3, CH_3I, DMF, reflux.

Monomeric building blocks **1d**, **1e** and **1l** were prepared according to Scheme 1. Carboxylic acid **1d** and amine **1e** were synthesized in four steps starting from pyridine-2,6-dicarboxylic acid **1a**. As shown in Scheme 1, pyridine-2,6-dicarboxylic acid underwent esterification in methanol to afford the diester methyl **1b** in a high yield of 96%. The second step involved the monohydrolysis of the diester to provide the monoacid **1c**. Several methods, such as using one equivalent of sodium hydroxide in cold or hot methanol or in cold or hot dioxane, or using one equivalent of potassium hydroxide in hot DMSO or in cold or hot methanol or in cold or hot dioxane were tried to obtain the product **1c**, however, most of the methods gave a low yield of the desired product with either the majority of starting material **1b** remaining unreacted or the dihydrolyzed product pyridine-2,6-dicarboxylic acid **1a** as the major product. The condition producing a 78% yield of

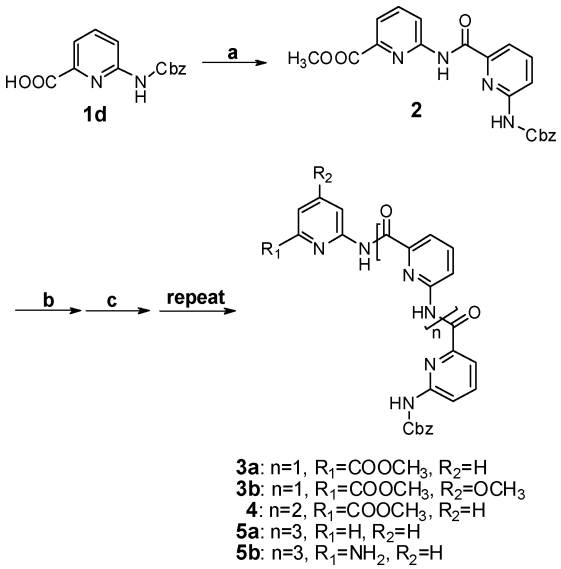

Scheme 2 Synthesis of aquafoldamers **2**–**5**. *Reagents and conditions*: (a) 4-methylmorpholine, ethyl chloroformate, THF–DMF, −10 to 0 °C, then **1c**; (b) NaOH, dioxane then 1 M HCl; (c) $(COCl)_2$, DMF, CH_2Cl_2, then **1e** (for **3a** and **4**), **1l** (for **3b**), 2-aminopyridine (for **5a**) or 2,6-diaminopyridine (for **5b**), Et_3N, CH_2Cl_2.

the monohydrolyzed product **1c** involves using one equivalent of potassium hydroxide in methanol and allowing the reaction to stir at room temperature overnight. The monoacid **1c** then underwent a Curtius rearrangement reaction to obtain monomer **1** in 65% yield. Compound **1c** first reacted with 4-methylmorpholine and ethyl chloroformate to give an active ester intermediate, which was then reacted with the nucleophile sodium azide to form the acyl azide intermediate. The acyl azide intermediate underwent Curtius rearrangement in the presence of benzyl alcohol to directly form the carbobenzyloxy (Cbz) protected amine **1**. Monomer acid **1d** was then obtained by subjecting monomer **1** to the hydrolysis by NaOH at room temperature overnight. The reaction must not be heated as, instead of **1d**, an amino acid product was obtained where the Cbz protecting group was deprotected under the basic condition at high temperatures. In order to obtain monomer amine **1e**, monomer **1** underwent a catalytic hydrogenation reaction using 10% palladium on activated carbon as the catalyst. The reaction was clean and efficient, giving a quantitative yield.

Monomer amine **1l** was obtained in eight steps starting from diethyl oxalate **1f**. Diacid **1g** was obtained after three steps: diethyl oxalate first underwent a Claisen condensation reaction with acetone using sodium ethoxide as the base, followed by a cyclization reaction in the presence of concentrated HCl and subsequent treatment with 10% aqueous ammonia solution. Esterification of diacid **1g** using thionyl chloride in methanol afforded diester methyl **1h**. The hydroxyl group, *meta* to the ester functionality, then underwent an alkylation reaction using potassium carbonate and methyl iodide to generate the alkylated product **1i** in 73% yield. Similar to the procedure to obtain monomer amine **1e**, the diester **1i** was subjected to a series of reactions consisting of monohydrolysis, Curtius rearrangement and catalytic hydrogenation to produce amine building block **1l**.

Following the elaboration of the synthetic routes for the efficient preparation of the various monomeric building blocks,

aquafoldamers **2–5** was then prepared according to Scheme 2 using a step-by-step approach with the various monomeric building blocks. The synthesis of dimer **2** started with monomer acid **1d** and monomer amine **1e** *via* an active ester intermediate.

Compound **1d** first reacted with 4-methylmorpholine and ethylchloroformate to form the active ester intermediate and the above *in situ* generated intermediate was then coupled with compound **1e** to yield dimer **2** in 52% yield. Hydrolysis of dimer **2** using NaOH at room temperature overnight yielded the dimer acid in 84% yield. An acid chloride was then generated from the dimer acid by treating the dimer acid with oxalyl chloride and a few drops of DMF in CH_2Cl_2 at room temperature. Trimers **3a** and **3b** were then synthesized by adding monomer amine **1e** and **1l**, respectively, to dimer acid chloride together with triethylamine. The higher oligomers were synthesized in the same fashion by allowing trimer **3a** to undergo a series of hydrolysis and coupling reactions to produce tetramer **4** and pentamers **5a** and **5b**. A unidirectional stepwise approach was used in the synthesis instead of a convergent approach where a higher oligomer such as a dimer acid is coupled to a dimer amine to synthesize a tetramer molecule, because (1) the higher oligomer amines have very poor solubilities in most organic solvents and (2) the H-bonding network in the higher oligomer amine is very strong, possibly resulting in a much lower reactivity of the amine in higher oligomers and hence giving a much lower yield. Therefore, for this particular class of oligoamides, a stepwise approach proves to be more efficient, in terms of both time and materials.

Solid-state structure of aquapentamer 5b

The crystal structures of **2**, **3**, **4** and **5a** have been recently reported by us.[3] Similar to these structures, the crystal structure of the pyridine-based aquapentamer **5b** (Fig. 1) shows an expected crescent-shaped helically folded structure as a result of an efficient backbone rigidification by the stabilizing forces from the continuous intramolecular H-bonding network (2.13–2.41 Å) formed from the inward-pointing amide protons and N-atoms on the pyridine rings. It could be observed that the helical backbone of **5b** requires about 4.3 repeating units to make up one helical turn, a helicity requirement also demanded by **5a**.[3a] The cavity enclosed by this set of aquapentamers **3–5** has a radius of about 2.6–3.3 Å, values that are slightly larger than ~ 2 Å pore radius found in the aquaporin water channel, suggesting that every crescent-shaped (*e.g.*, **3** and **4**) or helically folded (*e.g.*, **5**) aquafoldamer molecule is able to accommodate one or more than one water molecule in its

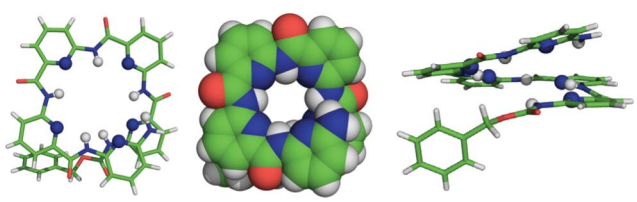

Fig. 1 Top and side views of crystal structure of the helically folded aquapentamer **5b**, illustrating the pyridine N-atoms (blue balls) and amide protons (gray balls) that participate in forming an intramolecular H-bonding network that induces the molecular backbone of **1** into a helical structure and encloses a water-binding helical cavity of about 2.7 Å in radius as measured from the cavity center to the center of the amide H-atom.

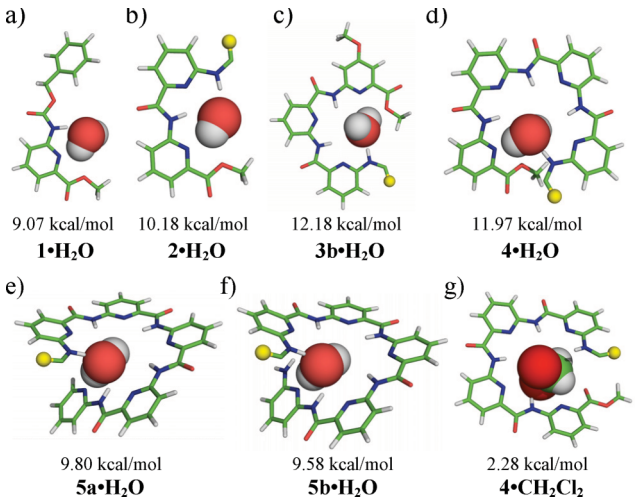

Fig. 2 Computationally determined structures for 1 : 1 water complexes **Aq**·H_2O (**Aq** = **1–5b**) at the B3LYP/6-311G+(2d,p) level in the gas phase. The corresponding binding energies per water molecule are shown below the structures. The crystal structure of **4** containing one CH_2Cl_2 molecule in its cavity is shown in (g). Both water and CH_2Cl_2 molecules are shown as CPK models. In the computed structures, all the water molecules are H-bonded to the amide H-atoms or pyridine N-atoms from the aquafoldamer hosts. Cbz groups are represented as the dummy atom in yellow.

cavity, respectively. More specifically, the water-binding abilities of this series of pyridine-derived cavity-enclosing aquapentamers can be proven by the water-containing crystal structure of **3b**, **5a** and **5b** (Fig. 3).

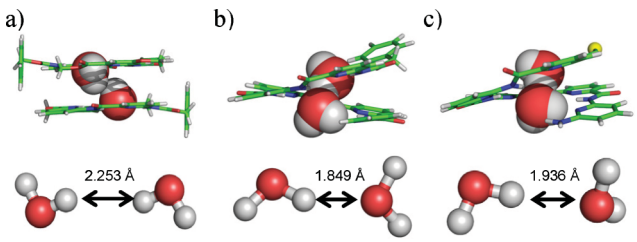

Fig. 3 Crystal structures for water complexes of (a) **3b**·H_2O, (b) **5a**·2H_2O and (c) **5b**·2H_2O, encapsulating both unconventional water dimer in **3b**·H_2O and conventional water dimers in **5a**·2H_2O and **5b**·2H_2O. Due to a difference in geometry, planar **3** binds only one water while helically folded **5a** and **5b** each trap two water molecules in their helical cavity. In (c), the Cbz group in **5b** is represented as the dummy atom in yellow. See Table 2 for the corresponding binding energies for forming water complexes and water dimers in these aquafoldamers.

Water complexes

Ab initio calculations performed on **1–5** at the level of B3LYP/6-311G+(2d,p) show that the 1 : 1 water complexes **Aq·H₂O** (**Aq** = **1–5b**) have a respective stability of 9.07 (**1**), 10.18 (**2**), 11.81 (**3a**), 12.18 (**3b**), 11.97 (**4**), 9.80 (**5a**), 9.58 (**5b**) kcal mol^{-1} with respect to its individual components (Fig. 2). Although the water complex **4**·H_2O is found to be energetically very favored (11.97 kcal mol^{-1}, Fig. 2d), **4** crystallographically encapsulates only CH_2Cl_2 molecules, rather than water molecules, in its cavity with a calculated binding energy of 2.28 kcal mol^{-1} per CH_2Cl_2 molecule

Table 1 Crystal growth conditions for oligomers **2–5**[a]

Slow diffusion with varying solvent pairs (1 : 1)				Slow evaporation	
2	CH_2Cl_2 : MeOH	**4**	CH_2Cl_2 : C_6H_{12}[b]	**3b**	CH_2Cl_2
5a	CH_2Cl_2 : C_6H_{12}[b]	**5b**	$CHCl_3$: EtOH		

[a] Crystals of **3a** could not be obtained under any the conditions tested, and oligomers have good solubilities in either CH_2Cl_2 or $CHCl_3$. [b] Cyclohexane.

(Fig. 2g). Further, the computationally determined water position in **3b** (Fig. 2c) differs from that found in its crystal structure (Fig. 3a). These discrepancies suggest that the computationally determined energetic favorability order can be possibly overridden by crystal packing effects.

Despite of repetitive efforts made to obtain the water complexes for these aquafoldamers, experimentally, it was not as straightforward. After screening numerous conditions involving various conditions of all the common organic solvents by method of either slow evaporation or diffusion, X-ray quality crystals of **2–5** were all obtained by their respective methods outlined in Table 1. Of further note is that both water-containing crystals of **3b** and **5a** were crystallized from water immiscible solvents, and only trace amounts of water molecules can be found in these crystallization conditions. And in the case of **4**, despite of having tried many conditions, even with using solvents that were saturated with water, water complexes of **4** could not be obtained. Except for crystals of dimer **2** containing no solvent or water molecules in its crystal lattice and tetramer **4** containing CH_2Cl_2 in its cavity, trimer **3b**, and pentamers **5a** and **5b** were all found to be capable of trapping water molecules in their interior cavities.

In both the water-containing crystal structures of **3b** and **5a** recently reported by us,[3b] the water molecules are stabilized in the cavities by intermolecular H-bonds of varying strengths with H-bond distances ranging from 1.92 to 2.91 Å. Due to its planar geometry, molecules of **3b** stack on top of each other to form a 1D columnar structure where every two molecules of **3b** trap an unconventional water dimer mediated by a H···H interaction (d_{H-H} = 2.253 Å, a distance that is ~ 0.15 Å less than twice the van der Waals radius of 1.20 Å for a hydrogen atom, Fig. 3a). Helically folded **5a** having a 3D-shaped cavity is able to accommodate two water molecules or one conventional water dimer mediated by a strong H-bond of 1.849 Å (Fig. 3b).[8]

In **5b**, ten intramolecular H-bonds (2.130–2.491 Å) are similarly found among pyridine N-atoms and amide H-atoms. These H-bonding forces lead to a helical conformation in **5b** that encloses a small cavity of ~2.7 Å in radius, measured from the centre of the cavity to the amide proton. A water dimer is thus trapped in the helical cavity of **5b** with intermolecular H-bonding distances between the water molecules and **5b** ranging from 1.93 to 2.76 Å. The water molecules further serve as *exo*-bidentate ligands, bridging the neighbouring two molecules of **5b** in a stair-like formation.

Computationally at the level of B3LYP/g-31G*, the H-bonding networks around the water molecules in **3b**, **5a** and **5b** provide a stabilizing energy of 7.61, 10.73 and 7.97 kcal mol^{-1}, respectively, for forming the water complexes (Table 2). The trapped water dimers in them have a respective binding energy of 2.22, 3.88 and 3.58 kcal mol^{-1} at the level of M062X/aug-cc-pVTZ. These water dimers are destabilized respectively by 2.99, 1.33 and 1.63 kcal mol^{-1} with respect to the binding energy of 5.21 kcal mol^{-1} for the most stable water dimer. This points to the instability of the trapped water dimers, formation of which is greatly facilitated by the stronger H-bonding network (Table 2) and a restricted cavity provided by these H-bond-rigidified aquafoldamers.

Table 2 Binding energies for water complexes and water dimers found in **3b**·H_2O, **5a**·2H_2O and **5b**·2H_2O in the gas phase

	Binding energy/kcal mol^{-1}		
	3b·H_2O	**5a**·2H_2O	**5b**·2H_2O
Aq + $m H_2O$ → **Aq**·$m H_2O$[a]	7.61	10.73	7.97
2H_2O → $(H_2O)_2$[b]	2.22	3.88	3.58

[a] For instance, **Aq** = **3b** and m = 1 for **3b**·H_2O. [b] For comparison, the computationally derived binding energy for the most stable water dimer is 5.21 kcal mol^{-1}.

One-dimensional ^{1}H NMR studies of the water complexes

The bound water molecules in the cavity of **2–5b** was further investigated by ^{1}H NMR in deuterated chloroform with varying water contents. More specifically, 5 mM of each of the oligoamide was prepared using (a) "normal" $CDCl_3$ directly taken from the bottle, (b) "wet" $CDCl_3$ saturated with water and (c) "dry" $CDCl_3$ dried by activated A4 molecular sieves. The corresponding ^{1}H NMR of the samples were recorded to examine the dependence of the chemical shifts of the amide protons on the water contents, which serves as an indicator on the water-binding ability of these molecules.

For **2**, it was observed that varying water contents essentially produces no changes among the NMR spectra recorded in "normal", "wet" and "dry" $CDCl_3$ (Fig. 4), indicating an inability for **2** to trap water molecules due to the open nature of its cavity. Accordingly, the amide protons in **2** do not H-bond to the water molecules, and thus no appreciable changes in the chemical shifts of the amide protons can be observed. This observation is consistent with the fact that no solvent or water molecules can be found in the crystal lattice of **2**.

Similar to **2**, the water content exhibits little effect on the chemical shifts of the amide protons in **4** (Fig. 4), which is crystallographically verified to be incapable of binding water molecules. But we found it difficult to explain this unusual behaviour by **4** as compared to other oligomers such as **3b** and **5** of the same series.

In contrast to **2** and **4** and consistent with their water-binding ability, significant differences were observed for ^{1}H NMR spectra of both aquafoldamers **3b** and **5b** in $CDCl_3$ containing varying water contents (Fig. 4). In general, the amide proton signals larger than 10.2 ppm shifted most downfield in the "wet" $CDCl_3$, while in "dry" $CDCl_3$, the signals shifted most upfield as compared to the "normal" and "wet" $CDCl_3$. The Cbz amide protons around 7.8 ppm for **3b** and 7.5 ppm for **5b** follow the same trend. These results were expected for aquafoldamers capable of binding water molecules because as the water contents in the solvent increases, the percentage of water complexes *vs.* "free" oligomer increases too, making the amide protons in average more deshielded and resulting in a downfield shift in the amide proton signals.

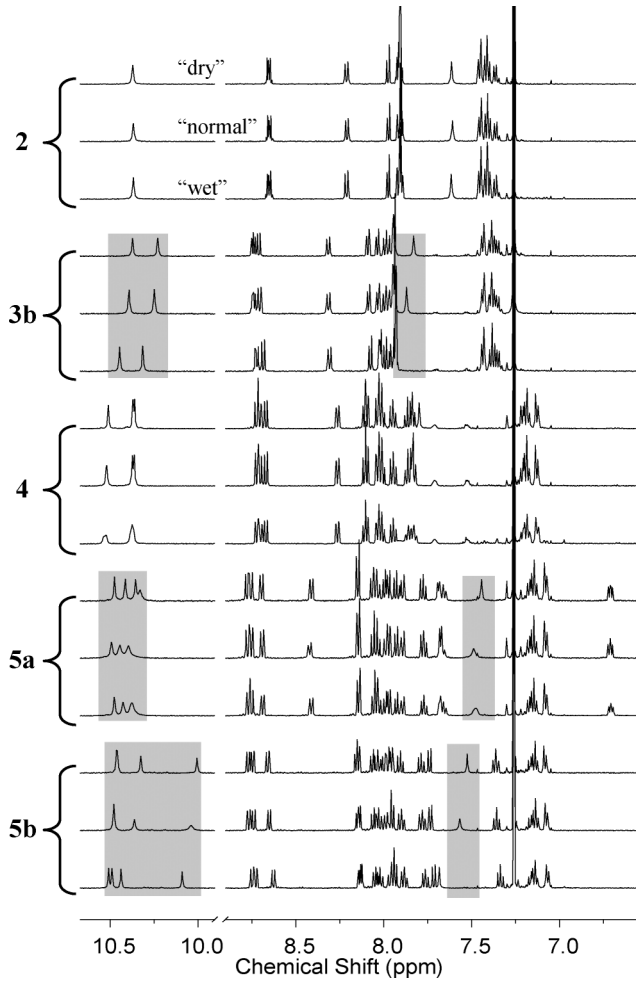

Fig. 4 Expanded ^{1}H NMR spectra of aromatic regions for **2–5** at 5 mM at 300 K in "dry", "normal" and "wet" $CDCl_3$ respectively shown from top to bottom. The shaded gray regions highlight differences in the chemical shifts of amide protons observed for **3b** and **5b**, and possibly also for **5a**, which are indicative of their water-binding ability.

Taking **3b** as an example, the proton signal for amide proton H_a shifted downfield from δ 10.34 ppm in "dry" $CDCl_3$ to 10.37 ppm in "normal" $CDCl_3$ and to 10.40 ppm in "wet" $CDCl_3$. The other two amide protons H_b and H_c display a similar trend (Table 3). Being similar in structure, the behaviour of the amide protons in **3a** was the same as those in **3b** in $CDCl_3$ containing varying water contents (Table 3).

As to **5a**, a small difference in ^{1}H NMR spectrum between "wet" and "dry' $CDCl_3$ does exist, but comparison of all the three spectrum including that in "normal" $CDCl_3$ gives inconclusive information on whether **5a** entraps water molecules in its cavity or not in solution, even though a water dimer is bound in its cavity in the solid state (Fig. 3b).

Cooling the samples from 300 to 223 K causes the most peak broadening in **4** and **5b** (Fig. 5), second most in **5a** and essentially no broadening in **2**, **3a** and **3b**, suggesting that aromatic π–π stacking interactions in **4** and **5b** are somewhat stronger that those in **5a**. As will be presented later in the paper, 2D NOESY experiments, *ab initio* calculations and ^{1}H NMR at varying concentrations were performed to probe for this unusual abnormality, and findings obtained are consistent with each other.

Table 3 The chemical shifts of amide protons in **3a** and **3b** in $CDCl_3$ of varying water contents

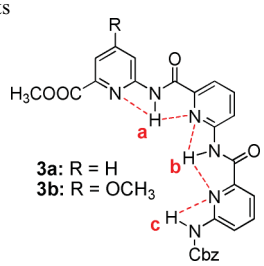

Oligoamide	Solvent	δ/ppm H_a	H_b	H_c
3a	Dry	10.37	10.23	7.83
	Normal	10.39	10.25	7.87
	Wet	10.45	10.31	> 7.90[a]
3b	Dry	10.34	10.22	7.83
	Normal	10.37	10.26	7.91
	Wet	10.40	10.29	> 7.92[a]

[a] Signals overlap with other protons.

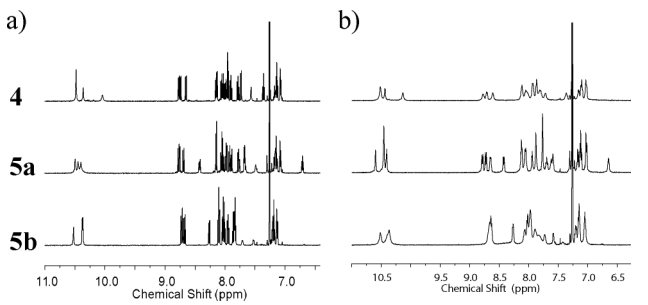

Fig. 5 ^{1}H NMR spectra of **4**, **5a** and **5b** at 5 mM in "normal" $CDCl_3$ at (a) 300 K and (b) 223 K, illustrating significant aggregations in **4** and **5b** while aggregation in **5a** is barely noticeable at 223 K.

2D NOESY studies of the water complexes

Given that the NOE contacts become detectable if the interatomic distance is less than 5 Å, a distance that is apparently longer that most of interatomic distances among H-atoms in water and water-containing aquafoldamers, observable NOE contacts among these H-atoms in close proximity are anticipated. Accordingly, these water complexes were further probed using 2D NOESY experiments. We further thought "freezing" all the atoms at low temperatures such as 223 K may make it possible to separate the "bound" water from "free" water,[7e] and to allow for an observation of NOE contacts between aquafoldamers and "bound" water molecules to provide direct evidences for the presence of bound water in the cavity of these aquafoldamers in solution.

2D NOESY experiments were then performed on trimer **3b** and pentamer **5a** at 223 K in "normal" $CDCl_3$. Expectedly, in addition to the signal from "free" water molecules, a new downfield-shifted peak ascribable to "bound" water molecules appeared in the ^{1}H NMR spectrum of **3b** (Fig. 6a). NOE contacts between the amide protons including that in Cbz group and protons from the water molecule bound in the cavity of **3b** were clearly seen (Fig. 6a). These NOE contacts are consistent with the results obtained from

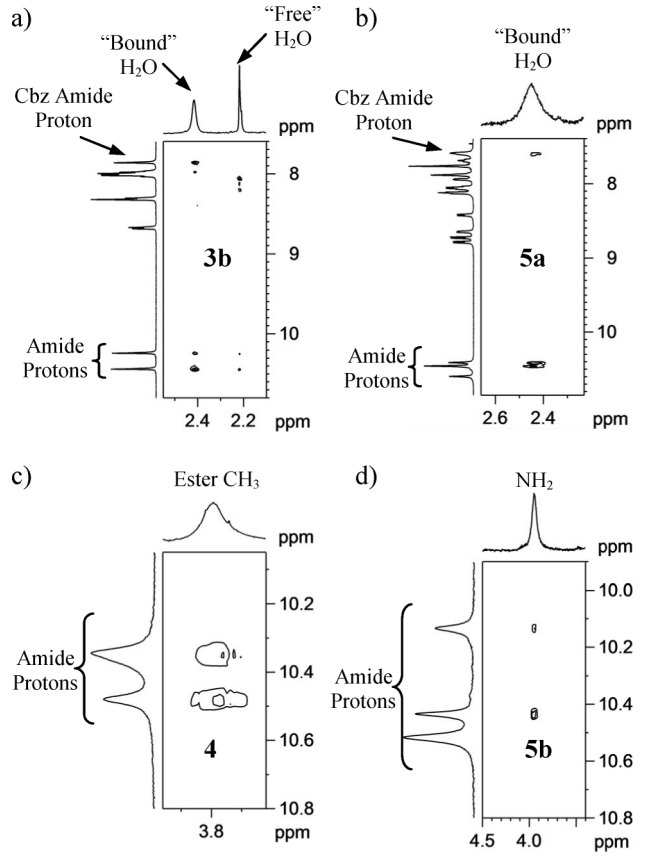

Fig. 6 Expanded 2D NOESY (223 K, "normal" $CDCl_3$, 500 MHz, mixing time = 500 ms) spectra of (a) **3b** at 10 mM, showing the NOE contacts between the bound water molecule and the amide protons of **3b**, (b) **5a** at 5 mM, showing the NOE contacts between the bound water molecule and the amide protons of **5a**, (c) **4** at 10 mM, showing the NOE contacts between the amide and ester methyl protons and (d) **5b** at 5 mM, showing the NOE contacts between the amide and amine protons.

the ^{1}H NMR studies carried out using $CDCl_3$ of varying water contents (Fig. 4) where the chemical shifts of the amide protons progressively downfield shift upon increasing water content in $CDCl_3$. For **5a**, similar NOE contacts between "bound" water and amide protons of **5a** were observed while it appears that no "free" water molecules are present in solution.

However, it still remains unclear to us as to why the 2D NOESY study of **5b** at 223 K in "normal" $CDCl_3$ did not give rise to any NOE contacts between water and **5b**. Nevertheless, two important interactions between the amide protons and the amine protons in **5b** were observed (Fig. 6d). One of these two NOE contacts is in good accord with the short distance of 2.768 Å between the end amine group and the amide proton involved in the three-center H-bonds at the other end, suggesting that the helical structure found in the solid state also persists in solution.

Surprisingly, strong NOE contacts between the amide protons and the end ester methyl protons in **4** were observed at 223 K (Fig. 6c). Crystallographically, conformers **4A** and **4B** are found with the methyl group staying away from the center of the cavity, resulting in the interatomic distances between methyl protons and amide protons excluding Cbz amide proton much larger than 5 Å. Only in **4C**, there exist at least two interatomic distances among methyl protons and the three amide protons H_a, H_b and H_c that are shorter than 5 Å, accounting for the observed NOE pattern in Fig. 6c. We therefore thought that at 223 K, **4** probably exists in a form of **4C** in solution where the ester methyl protons point into its cavity, thus preventing the water molecule from entering the cavity.

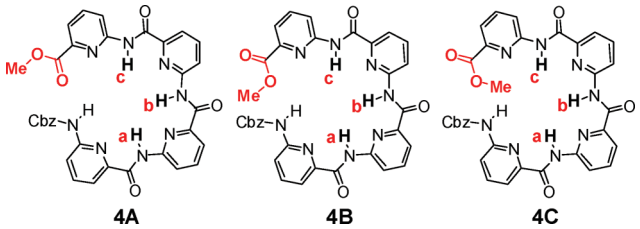

Ab initio studies of the conformers of 4 and dimeric structures

Presumably due to the predominant occurrence of conformer **4C** in solution, water molecules cannot enter the cavity in **4**. *Ab initio* computations were then carried out to investigate the likelihood of **4C** as the major conformer with respect to the crystallographically found **4A** and **4B** by comparing their relative stabilities on the basis of the computationally derived relative energies among them.

Contrary to what we hypothesized above, calculations using density functional theory at the level of B3LYP/6-31G* with a polarized continuum model (PCM) in chloroform at 223 K on different conformers of **4A–4C** with its ester methyl protons in different positions (Fig. 7) reveals conformer **4A1** found in the solid state to be computationally the most stable, marginally more stable than **4B** that is also found in the solid state by 0.55 kcal mol^{-1}, and significantly much more stable than the "desired" conformers **4C** (Fig. 7d–e) by at least 7.45 kcal mol^{-1}. With these differences in energy, either **4C1** or **4C2** is less than 10-millionth of either **4A1** or **4B**. In all the modeled structures, the Cbz groups are roughly perpendicular to the macrocyclic plane. Further, it can be seen that methyl group in the more stable states tends to stay away from the cavity by pointing outward (**4A1**/**4B** *vs.* **4C1**) and slightly upward (**4A1** *vs.* **4A2**, and **4C1** *vs.* **4C2**), rather than inward and down to the cavity.

In order to account for the observations noted in the variable-temperature ^{1}H NMR (Fig. 5a) and 2D NOESY experiments (Fig. 6c) that signify a strong aggregation in **4** and close proximity between its ester methyl protons and amide protons, the next most possible logical explanation would be that **4** exists as a self-trapping dimer with having its methyl protons pointing or protruding into the cavity of another molecule of **4**. The extensive interactions involving feeble intermolecular H-bonds and aromatic π–π stackings possibly would bring two molecules of **4** much closer together, occupying mutual cavities and thus preventing water molecules from entering the cavities. This dimeric structure may constitute a good model for explaining the obtained abnormal findings. Our calculation using a Dreiding force field[11] indeed demonstrates a possibility of dimerization involving two molecules of **4** with a very substantial binding energy of 80.69 kcal mol^{-1} per dimer (Fig. 8a–8c). This is a result of three types of stabilizing intermolecular forces provided largely by (1) extensive H-bonds (Fig. 8b) and (2) aromatic π–π stacking, and (3) by van der Waals interactions to a good extent as suggested by a nearly perfect match in size between the ester group and the cavity (Fig. 8c). From the computed dimeric structures, it can be seen that the

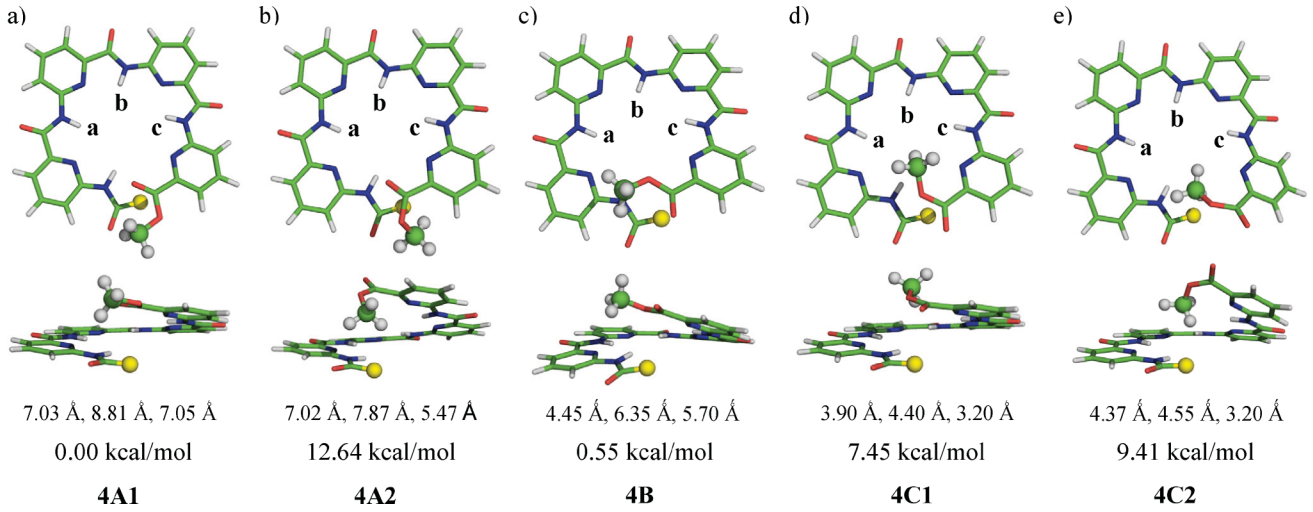

Fig. 7 Top and side views of the computationally optimized geometries of varying conformers for **4** at BYLYP/6-31G* level in $CHCl_3$ at 223 K. The shortest distances among methyl protons and amide protons H_a, H_b and H_c are shown below the structures. Shown below the distances are the relative energies in kcal mol^{-1} among the five conformers normalized against the most stable conformer **4A1**. Methyl protons and methyl carbon are in gray and green balls, respectively, with the Cbz group represented as a yellow dummy atom.

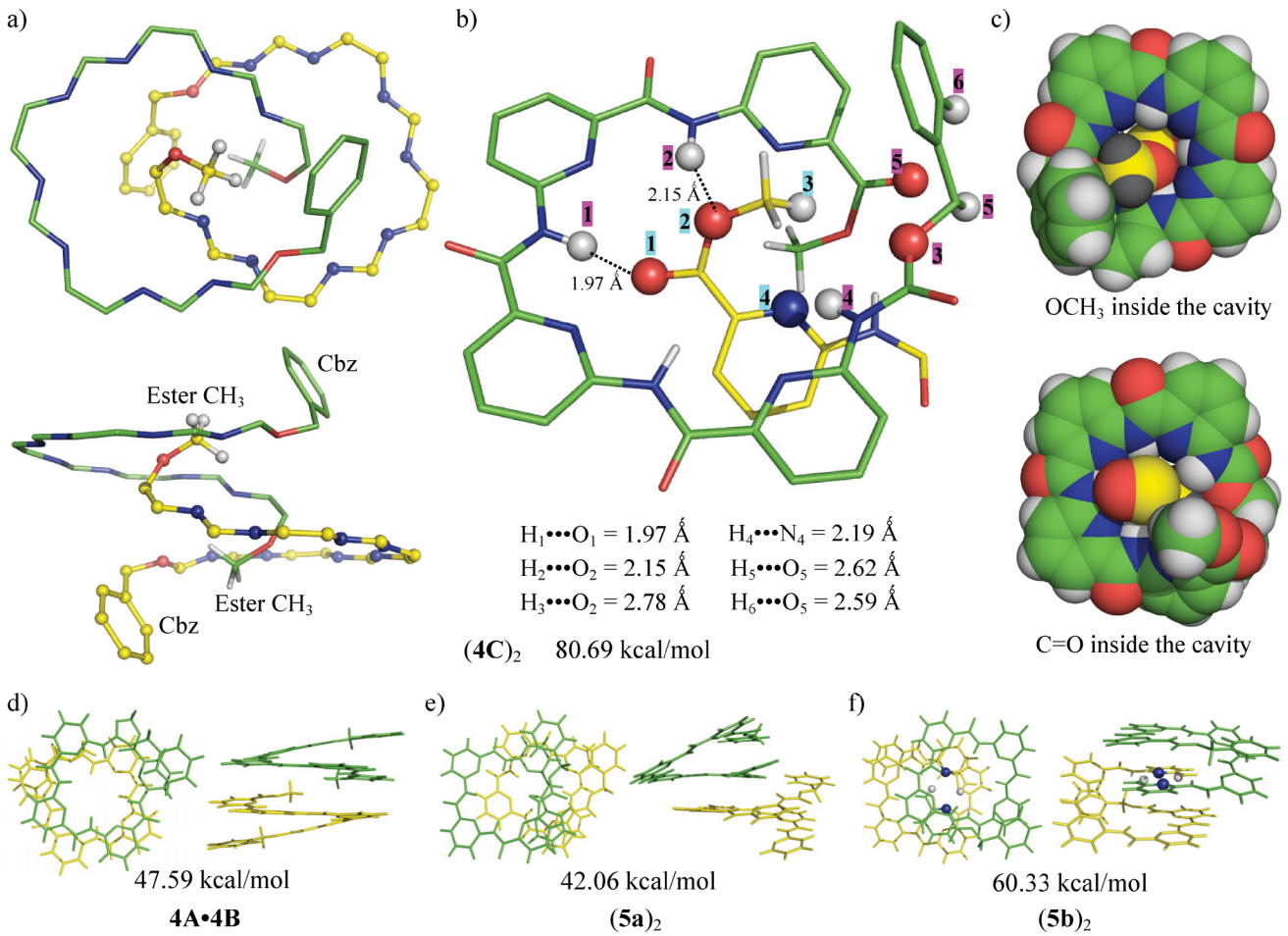

Fig. 8 Top and side views of the computationally optimized geometries for dimeric structures of (a–c) $(4C)_2$, (d) **4A**·**4B**, (e) $(5a)_2$ and (f) $(5b)_2$ using the Dreiding field force in the gas phase. In (a) a skeleton representation of $(4C)_2$ where only the inner atoms are shown with carbon atoms in green and yellow, respectively. In (b), the fragment at the ester end of the second molecule is shown with carbon atoms in yellow, and with only one of two identical sets of H-bonds of <2.8 Å. In (c), front and back views of the fragmented ester group inside the cavity ($COOCH_3$, H, C and O as black, yellow and red balls) from the second molecule are presented as a CPK model, illustrating an excellent fit of the ester group into the cavity enclosed by **4C**. In (f), the two H-atoms and N-atoms involved in H-bonds at the amine end are shown in gray and blue balls, respectively. The binding energy for dimerization is shown in kcal mol^{-1} below the structures. Clearly, **4C** exhibits the highest energetic gain by self-dimerizing.

overlap involving helical aromatic backbones is the best in dimer **4A**·**4B**. Due to the existence of extensive H-bonds in $(\mathbf{4C})_2$, two strong H-bonds in $(\mathbf{5b})_2$ and longer backbones in **5a** and **5b**, the energetic gain among the four dimers increase in the order of $(\mathbf{5a})_2$ < **4A**·**4B** < $(\mathbf{5b})_2$ < $(\mathbf{4C})_2$. This order explains well the aggregation behaviors displayed by **4**, **5a** and **5b** (Fig. 5). Further, since **4C** clearly exhibits a much higher energetic gain (80.69 kcal mol^{-1}) by self-dimerizing with respect to the heterodimer **4A**·**4B** (47.59 kcal mol^{-1}) found in the solid state, it is likely that **4C**, not **4A** or **4B**, is the predominant conformation adopted by **4** in solution, and increasingly dimerizes upon decreasing the temperature. On the basis of the computed structures, the shortest distances between ester methyl protons and amides protons *a*, *b* and *c* are 3.65, 4.76 and 2.76 Å, respectively, accounting for both the observation of strong NOEs between methyl protons and amide protons (Fig. 6c) and why tetramer **4**, seemingly possessing a water-binding cavity, does not bind water molecules in solution (Fig. 4).

In the computed dimeric structure of $(\mathbf{4C})_2$, the two ester methyl groups are surrounded by aromatic benzene rings, and their chemical shift will be affected by these aromatic ring currents. A concentration-dependant analysis of ^{1}H NMR of **4** that may be composed of a mixture of monomer and dimer in varying ratios in $CDCl_3$ demonstrates an upfield shift for the two methyl groups from 3.883 to 3.846 upon increasing the concentration from 1 to 20 mM (Fig. 9a). For comparison, the same analysis of trimer **3a** shows a very small upfield shift from 3.916 to 3.904 ppm for its methyl group within the same concentration range (Fig. 9b). Since higher concentrations favor the formation of more dimer $(\mathbf{4C})_2$, a decrease in chemical shift at higher concentrations suggests the methyl groups to be more shielded from the NMR magnetic field. If the self-trapping dimerization model proposed in Fig. 8a–c is essentially correct or resembles its real structure to a very good extent, the benzene rings surrounding the methyl groups should produce a shielding rather than deshielding effect in order to explain the observed ^{1}H NMR shift for methyl groups. In this regard, we carried out the computational investigations of the chemical shifts of the methyl groups in monomer **4C** and dimer $(\mathbf{4C})_2$. The structure of dimer $(\mathbf{4C})_2$ was optimized using the Dreiding force field as shown in Fig. 8a–c with its NMR chemical shift values calculated at the B3LYP/6-31G* level in both gas phase and chloroform (Table 4). Monomer **4C** was taken out of the optimized dimer structure and subjected to the same treatment. Our calculations indeed show that **4C** in 100% dimer state experiences a very substantial shielding effect by the nearby aromatic ring currents, leading to a NMR chemical shift of 2.21 ppm in chloroform as compared to **4C** in 100% monomer state with a chemical shift of 4.23 ppm. Although a difference in chemical shift of methyl group between **4C** and $(\mathbf{4C})_2$ may not be as large as 2.02 ppm in chloroform, a general trend where dimerization involving two molecules of **4C** causes their methyl protons to experience more shielding effects and thus to have a smaller chemical shift value with respect to the monomeric **4C** largely should hold true, at least computationally.

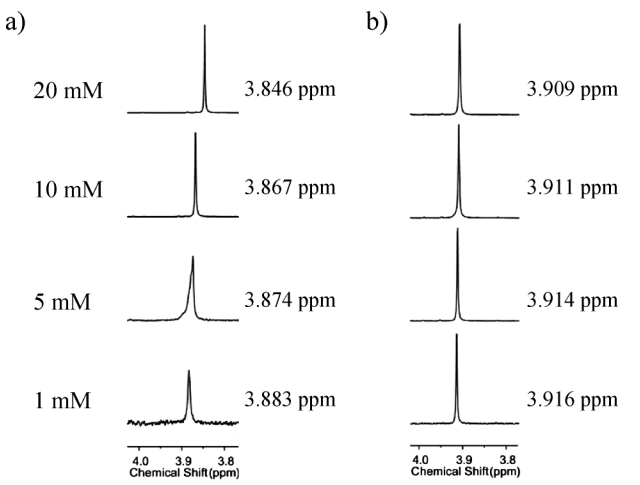

Fig. 9 ^{1}H NMR spectra ($CDCl_3$, 500 MHz, 298 K) for ester methyl protons from (a) **4** and (b) **3a**, illustrating comparably different changes in concentration-dependant chemical shift between **4** and **3a** within the same concentration range of 1–20 mM.

Table 4 Computationally calculated chemical shifts in ppm with TMS as the reference for the ester methyl protons from monomer **4C** and dimer $(\mathbf{4C})_2$ in both gas phase and chloroform

	Dreiding force field[a]			
	Gas phase		Chloroform	
	4C	$(\mathbf{4C})_2$	**4C**	$(\mathbf{4C})_2$
δ/ppm	4.15	1.93	4.23	2.21

[a] Structures are optimized using the Dreiding force field, followed by calculating chemical shifts using B3LYP/6-31G*.

Conclusions

In this article, we describe our detailed studies on the various aspects of water-binding aquafoldamers, particularly, aquatrimer **3b** and aquapentamers **5a** and **5b**. While a short pyridine-based **3b** is found to encapsulate a water molecule in its nearly planar cavity and subsequently traps a unconventional water dimer, a 3D-shaped helical cavity as in longer oligomers such as **5a** and **5b** is able to accommodate two water molecules that dimerize *via* a strong intermolecular H-bond of different strengths. As a result of a structural rigidity imposed by these aquafoldamers onto the water molecules, these water dimers are destabilized by 1.33–2.99 kcal mol^{-1} with regard with the most stable "unbound" water dimer. Consistent with these solid-state structures, investigations by both 1D ^{1}H NMR using $CDCl_3$ containing varying water contents and 2D NOESY studies at low temperature provide a good support to the ability of these aquafoldamers to bind water molecules in solution. We envisioned that by elongating the helical backbones either covalently or non-covalently, enlarged or longer 3D-shaped cavities can be created for encapsulating larger water clusters of diverse topographies in their interiors. On the other hand, aided by computational molecular modelling, a self-trapping dimerization model involving two molecules of **4** protruding into mutual cavities is proposed, which is consistent with the observed (1) inability of **4** to bind water in solution state, (2) abnormal aggregation in **4**, (3) strong NOE contacts that suggest a close proximity between ester methyl protons and amide protons in **4**, and (4) a progressive downfield shifting of ester methyl protons in **4** upon increasing the concentration. Whether this dimeric structure can

be found in the solid state or not is a subject worth of further investigation.

Acknowledgements

Financial support by A*STAR BMRC research consortia (R-143-000-388-305 to H. Z.) and by Environment and Water Industry Development Council and Economic Development Board (SPORE, COY-15-EWI-RCFSA/N197-1 to H. Z.).

Notes and references

1 (*a*) A. S. Verkman, *J. Cell Sci.*, 2011, **124**, 2107; (*b*) P. Agre, M. Bonhivers and M. J. Borgnia, *J. Biol. Chem.*, 1998, **273**, 14659; (*c*) M. Borgnia, S. Nielsen, A. Engel and P. Agre, *Annu. Rev. Biochem.*, 1999, **68**, 425; (*d*) G. M. Preston, T. P. Carroll, W. B. Guggino and P. Agre, *Science*, 1992, **256**, 385.

2 (*a*) L. Strand, S. E. Moe, T. T. Solbu, M. Vaadal and T. Holen, *Biochemistry*, 2009, **48**, 5785; (*b*) B. Otto, N. Uehlein, S. Sdorra, M. Fischer, M. Ayaz, X. Belastegui-Macadam, M. Heckwolf, M. Lachnit, N. Pede, N. Priem, A. Reinhard, S. Siegfart, M. Urban and R. Kaldenhoff, *J. Biol. Chem.*, 2010, **285**, 31253; (*c*) J. B. Heymann, P. Agre and A. Engel, *J. Struct. Biol.*, 1998, **121**, 191.

3 (*a*) W. Q. Ong, H. Q. Zhao, Z. Y. Du, J. Z. Y. Yeh, C. L. Ren, L. Z. W. Tan, K. Zhang and H. Q. Zeng, *Chem. Commun.*, 2011, **47**, 6416; (*b*) W. Q. Ong, H. Q. Zhao, X. Fang, S. Woen, F. Zhou, W. L. Yap, H. B. Su, S. F. Y. Li and H. Q. Zeng, *Org. Lett.*, 2011, **13**, 3194.

4 (*a*) L. X. Song, L. Bai, X. M. Xu, J. He and S. Z. Pan, *Coord. Chem. Rev.*, 2009, **253**, 1276; (*b*) K. Ono, K. Tsukamoto, R. Hosokawa, M. Kato, M. Suganuma, M. Tomura, K. Sako, K. Taga and K. Saito, *Nano Lett.*, 2009, **9**, 122; (*c*) W. Si, X.-B. Hu, X.-H. Liu, R. Fan, Z. Chen, L. Weng and J.-L. Hou, *Tetrahedron Lett.*, 2011, **52**, 2484; (*d*) Z. Zhang, Y. Luo, J. Chen, S. Dong, Y. Yu, Z. Ma and F. Huang, *Angew. Chem., Int. Ed.*, 2011, **50**, 1397; (*e*) Z. Zhang, Y. Luo, B. Xia, C. Han, Y. Yu, X. Chen and F. Huang, *Chem. Commun.*, 2011, **47**, 2417; (*f*) Z. Zhang, B. Xia, C. Han, Y. Yu and F. Huang, *Org. Lett.*, 2010, **12**, 3285.

5 (*a*) J. R. Moon, A. J. Lough, Y. T. Yoon, Y. I. Kim and J. C. Kim, *Inorg. Chim. Acta*, 2010, **363**, 2682; (*b*) M. H. Mir, L. Wang, M. W. Wong and J. J. Vittal, *Chem. Commun.*, 2009, 4539.

6 For some recent reviews on foldamers, see: (*a*) S. H. Gellman, *Acc. Chem. Res.*, 1998, **31**, 173; (*b*) K. D. Stigers, M. J. Soth and J. S. Nowick, *Curr. Opin. Chem. Biol.*, 1999, **3**, 714; (*c*) B. Gong, *Chem.–Eur. J.*, 2001, **7**, 4336; (*d*) D. J. Hill, M. J. Mio, R. B. Prince, T. S. Hughes and J. S. Moore, *Chem. Rev.*, 2001, **101**, 3893; (*e*) R. P. Cheng, S. H. Gellman and W. F. DeGrado, *Chem. Rev.*, 2001, **101**, 3219; (*f*) M. S. Cubberley and B. L. Iverson, *Curr. Opin. Chem. Biol.*, 2001, **5**, 650; (*g*) A. R. Sanford and B. Gong, *Curr. Org. Chem.*, 2003, **7**, 1649; (*h*) A. R. Sanford, K. Yamato, X. Yang, L. Yuan, Y. Han and B. Gong, *Eur. J. Biochem.*, 2004, **271**, 1416; (*i*) C. Schmuck, *Angew. Chem., Int. Ed.*, 2003, **42**, 2448; (*j*) I. Huc, *Eur. J. Org. Chem.*, 2004, 17; (*k*) R. P. Cheng, *Curr. Opin. Struct. Biol.*, 2004, **14**, 512; (*l*) G. Licini, L. J. Prins and P. Scrimin, *Eur. J. Org. Chem.*, 2005, 969; (*m*) Z. T. Li, J. L. Hou, C. Li and H. P. Yi, *Chem.–Asian J.*, 2006, **1**, 766; (*n*) X. Li and D. Yang, *Chem. Commun.*, 2006, 3367; (*o*) C. Z. Li, X. K. Jiang, Z. T. Li, X. Gao and Q. R. Wang, *Chin. J. Org. Chem.*, 2007, **27**, 188; (*p*) C. M. Goodman, S. Choi, S. Shandler and W. F. DeGrado, *Nat. Chem. Biol.*, 2007, **3**, 252; (*q*) B. Gong, *Acc. Chem. Res.*, 2008, **41**, 1376; (*r*) D. Haldar, *Curr. Org. Synth.*, 2008, **5**, 61; (*s*) Z. T. Li, J. L. Hou and C. Li, *Acc. Chem. Res.*, 2008, **41**, 1343; (*t*) B. Baptiste, F. Godde and I. Huc, *ChemBioChem*, 2009, **10**, 1765; (*u*) W. S. Horne and S. H. Gellman, *Acc. Chem. Res.*, 2008, **41**, 1399; (*v*) I. Saraogi and A. D. Hamilton, *Chem. Soc. Rev.*, 2009, **38**, 1726; (*w*) D. Haldar and C. Schmuck, *Chem. Soc. Rev.*, 2009, **38**, 363; (*x*) X. Zhao and Z. T. Li, *Chem. Commun.*, 2010, **46**, 1601.

7 (*a*) V. Berl, I. Huc, R. Khoury and J.-M. Lehn, *Chem.–Eur. J.*, 2001, **7**, 2798; (*b*) V. Berl, I. Huc, R. G. Khoury and J.-M. Lehn, *Chem.–Eur. J.*, 2001, **7**, 2810; (*c*) I. Huc, V. Maurizot, H. Gornitzka and J.-M. Leger, *Chem. Commun.*, 2002, 578; (*d*) J. Garric, J.-M. Léger and I. Huc, *Angew. Chem., Int. Ed.*, 2005, **44**, 1954; (*e*) J. Garric, J.-M. Léger and I. Huc, *Chem.–Eur. J.*, 2007, **13**, 8454.

8 M. C. Bheda, J. S. Merola, W. A. Woodward, V. J. Vasudevan and H. W. Gibson, *J. Org. Chem.*, 1994, **59**, 1694.

9 For some selected examples of aromatic foldamers, see: (*a*) Y. Hamuro, S. J. Geib and A. D. Hamilton, *Angew. Chem., Int. Ed. Engl.*, 1994, **33**, 446; (*b*) Y. Hamuro, S. J. Geib and A. D. Hamilton, *J. Am. Chem. Soc.*, 1996, **118**, 7529; (*c*) Y. Hamuro, S. J. Geib and A. D. Hamilton, *J. Am. Chem. Soc.*, 1997, **119**, 10587; (*d*) V. Berl, I. Huc, R. G. Khoury, M. J. Krische and J. M. Lehn, *Nature*, 2000, **407**, 720; (*e*) V. Berl, I. Huc, R. Khoury and J.-M. Lehn, *Chem.–Eur. J.*, 2001, **7**, 2810; (*f*) E. Kolomiets, V. Berl, I. Odriozola, A. M. Stadler, N. Kyritsakas and J. M. Lehn, *Chem. Commun.*, 2003, 2868; (*g*) J. Zhu, R. D. Parra, H. Q. Zeng, E. Skrzypczak-Jankun, X. C. Zeng and B. Gong, *J. Am. Chem. Soc.*, 2000, **122**, 4219; (*h*) B. Gong, H. Q. Zeng, J. Zhu, L. H. Yuan, Y. H. Han, S. Z. Cheng, M. Furukawa, R. D. Parra, A. Y. Kovalevsky, J. L. Mills, E. Skrzypczak-Jankun, S. Martinovic, R. D. Smith, C. Zheng, T. Szyperski and X. C. Zeng, *Proc. Natl. Acad. Sci. U. S. A.*, 2002, **99**, 11583; (*i*) L. H. Yuan, H. Q. Zeng, K. Yamato, A. R. Sanford, W. Feng, H. S. Atreya, D. K. Sukumaran, T. Szyperski and B. Gong, *J. Am. Chem. Soc.*, 2004, **126**, 16528; (*j*) X. W. Yang, L. H. Yuan, K. Yamamoto, A. L. Brown, W. Feng, M. Furukawa, X. C. Zeng and B. Gong, *J. Am. Chem. Soc.*, 2004, **126**, 3148; (*k*) A. M. Zhang, Y. H. Han, K. Yamato, X. C. Zeng and B. Gong, *Org. Lett.*, 2006, **8**, 803; (*l*) W. Feng, K. Yamato, L. Q. Yang, J. Ferguson, L. J. Zhong, S. L. Zou, L. H. Yuan, X. C. Zeng and B. Gong, *J. Am. Chem. Soc.*, 2009, **131**, 2629; (*m*) P. S. Corbin, S. C. Zimmerman, P. A. Thiessen, N. A. Hawryluk and T. J. Murray, *J. Am. Chem. Soc.*, 2001, **123**, 10475; (*n*) H. Jiang, J.-M. Leger and I. Huc, *J. Am. Chem. Soc.*, 2003, **125**, 3448; (*o*) D. Haldar, H. Jiang, J. M. Leger and I. Huc, *Angew. Chem., Int. Ed.*, 2006, **45**, 5483; (*p*) Q. Gan, C. Y. Bao, B. Kauffmann, A. Grelard, J. F. Xiang, S. H. Liu, I. Huc and H. Jiang, *Angew. Chem., Int. Ed.*, 2008, **47**, 1715; (*q*) J. L. Hou, X. B. Shao, G. J. Chen, Y. X. Zhou, X. K. Jiang and Z. T. Li, *J. Am. Chem. Soc.*, 2004, **126**, 12386; (*r*) C. Li, S.-F. Ren, J.-L. Hou, H.-P. Yi, S.-Z. Zhu, X.-K. Jiang and Z.-T. Li, *Angew. Chem., Int. Ed.*, 2005, **44**, 5725; (*s*) J.-L. Hou, H.-P. Yi, X.-B. Sha, C. Li, Z.-Q. Wu, X.-K. Jian, L.-Z. Wu, C.-H. Tung and Z.-T. Li, *Angew. Chem., Int. Ed.*, 2006, **45**, 796; (*t*) W. Cai, G. T. Wang, Y. X. Xu, X. K. Jiang and Z. T. Li, *J. Am. Chem. Soc.*, 2008, **130**, 6936; (*u*) D. Kanamori, T. A. Okamura, H. Yamamoto and N. Ueyama, *Angew. Chem., Int. Ed.*, 2005, **44**, 969; (*v*) X. Li, C. L. Zhan, Y. B. Wang and J. N. Yao, *Chem. Commun.*, 2008, 2444; (*w*) J. Rebek, *Acc. Chem. Res.*, 2009, **42**, 1660; (*x*) Q. Gan, Y. Ferrand, C. Bao, B. Kauffmann, A. Grélard, H. Jiang and I. Huc, *Science*, 2011, **331**, 1172.

10 For some selected examples of aromatic foldamers, see: (*a*) B. Qin, X. Y. Chen, X. Fang, Y. Y. Shu, Y. K. Yip, Y. Yan, S. Y. Pan, W. Q. Ong, C. L. Ren, H. B. Su and H. Q. Zeng, *Org. Lett.*, 2008, **10**, 5127; (*b*) Y. Yan, B. Qin, Y. Y. Shu, X. Y. Chen, Y. K. Yip, D. W. Zhang, H. B. Su and H. Q. Zeng, *Org. Lett.*, 2009, **11**, 1201; (*c*) B. Qin, C. L. Ren, R. J. Ye, C. Sun, K. Chiad, X. Y. Chen, Z. Li, F. Xue, H. B. Su, G. A. Chass and H. Q. Zeng, *J. Am. Chem. Soc.*, 2010, **132**, 9564; (*d*) Y. Yan, B. Qin, C. L. Ren, X. Y. Chen, Y. K. Yip, R. J. Ye, D. W. Zhang, H. B. Su and H. Q. Zeng, *J. Am. Chem. Soc.*, 2010, **132**, 5869; (*e*) B. Qin, C. Sun, Y. Liu, J. Shen, R. J. Ye, J. Zhu, X.-F. Duan and H. Q. Zeng, *Org. Lett.*, 2011, **13**, 2270; (*f*) B. Qin, W. Q. Ong, R. J. Ye, Z. Y. Du, X. Y. Chen, Y. Yan, K. Zhang, H. B. Su and H. Q. Zeng, *Chem. Commun.*, 2011, **47**, 5419; (*g*) B. Qin, S. Shen, C. Sun, Z. Y. Du, K. Zhang and H. Q. Zeng, *Chem.–Asian J.*, 2011, **6**, 3298; (*h*) C. L. Ren, S. Y. Xu, J. Xu, H. Y. Chen and H. Q. Zeng, *Org. Lett.*, 2011, **13**, 3840; (*i*) C. L. Ren, F. Zhou, B. Qin, R. J. Ye, S. Shen, H. B. Su and H. Q. Zeng, *Angew. Chem., Int. Ed.*, 2011, **50**, 10612; (*j*) C. L. Ren, V. Maurizot, H. Q. Zhao, J. Shen, F. Zhou, W. Q. Ong, Z. Y. Du, K. Zhang, H. B. Su and H. Q. Zeng, *J. Am. Chem. Soc.*, 2011, **133**, 13930; (*k*) Z. Y. Du, C. L. Ren, R. J. Ye, J. Shen, Y. J. Lu, J. Wang and H. Q. Zeng, *Chem. Commun.*, 2011, **47**, 12488.

11 S. L. Mayo, B. D. Olafson and W. A. Goddard III, *J. Phys. Chem.*, 2009, **94**, 8897.

